Plasmon-cyclotron resonance in two-dimensional electron gas confined at the $GaN/Al_xGa_{1-x}N$ interface

Agnieszka Wolos
Institute of Semiconductor and Solid State Physics, Johannes Kepler Universität, Altenbergerstrasse 69, A-4040 Linz, Austria and Institute of Physics, Polish Academy of Sciences, Aleja Lotnikow 32/46, 02-668 Warszawa, Poland

Wolfgang Jantsch
Institute of Semiconductor and Solid State Physics, Johannes Kepler Universität, Altenbergerstrasse 69, A-4040 Linz, Austria

Krzysztof Dybko and Zbyslaw Wilamowski
Institute of Physics, Polish Academy of Sciences, Aleja Lotnikow 32/46, 02-668 Warszawa, Poland

Czeslaw Skierbiszewski
Institute of High Pressure Physics, Polish Academy of Sciences, ulica Sokolowska 29/37, 01-142 Warszawa, Poland
(Received 13 April 2007; revised manuscript received 23 May 2007; published 2 July 2007)

Edge magnetoplasma modes are studied in the two-dimensional electron gas confined at the $GaN/Al_xGa_{1-x}N$ interface using standard microwave resonance spectroscopy. The position and shape of the resonance line are described by the theory for the dimension-dependent plasmon-cyclotron coupling and the Drude model of momentum relaxation. The analysis of the resonance line shape provides a contactless method for the determination of the sheet electron concentration and the mobility of the two-dimensional electron gas. In addition, we observe Shubnikov–de Haas oscillations using the same microwave resonance spectrometry. We compare values for the cyclotron and quantum mobilities obtained from the plasmon-cyclotron linewidth and the magnetic field dependence of the Shubnikov–de Haas signal, respectively.

DOI: 10.1103/PhysRevB.76.045301 PACS number(s): 73.40.Kp, 76.30.Pk, 76.40.+b

I. INTRODUCTION

Early work on the two-dimensional electron gas (2DEG) in silicon inversion layers[1] or in GaAs-based heterostructures[2–5] showed that when the plasma frequency of the 2D electrons approaches the cyclotron frequency, the two modes hybridize into a coupled excitation. Neglecting retardation effects[4] for a disk-shaped sample, the plasmon-cyclotron spectrum is characterized by two branches, which at zero magnetic field converge at the frequency of the plasma oscillations. For high magnetic fields, the upper magnetoplasma branch, a cyclotronlike mode, asymptotically approaches the cyclotron frequency, while the lower branch, the so-called edge mode, approaches zero.

In order to correctly evaluate parameters from the cyclotron resonance spectrum, particularly the value of the effective mass, it is important to consider the plasmon-cyclotron coupling. The latter becomes important when the resonance frequency in the experiment is comparable to both the plasma and the cyclotron frequency.

In this paper, we present the results for the two-dimensional electron gas confined at the GaN/AlGaN interface. Using a standard electron spin resonance (ESR) spectrometer, we have observed a broad line resembling a cyclotron resonance, whose position corresponds, however, to an apparent cyclotron mass of $1.3m_0$. This value is far from the effective mass of conduction electrons in GaN, $0.2m_0$, previously determined for GaN/AlGaN heterostructures in cyclotron resonance experiments.[6–10] The shift of the observed line indicates plasmon-cyclotron coupling, and this is further corroborated by the detailed analysis of the spectra. We show that the observed resonance is due to the edge magnetoplasma mode.

Plasmon-cyclotron coupling has been extensively studied in GaAs-based heterostructures, for which high sheet electron mobilities of up to 10^6 cm^2/V s can be achieved.[3–5] The high mobility of the 2D electrons is an essential prerequisite for studying this type of excitations, as the electron scattering time can be directly related to the linewidth of the resonance peak.[11] The higher the mobility of the 2D electrons, the narrower the linewidth.

Mobilities reaching 10^6 cm^2/V s have not been achieved yet for GaN/AlGaN. However, thanks to the progress in GaN-based technology, due in particular to the use of native GaN substrates, it is possible to obtain samples with mobilities as high as 10^4–10^5 cm^2/V s.[12,13] Such samples have been used for studying properties of the two-dimensional magnetoplasma in this paper.

II. SAMPLES AND EXPERIMENTAL DETAILS

Heterostructures were grown on semi-insulating GaN bulk substrates[14] on the Ga-polarity (0001) surface by plasma-assisted molecular beam epitaxy (MBE). The surface of the substrates was prepared for the growth by the standard method including mechanical polishing followed by mechanochemical polishing. The MBE-grown heterostructure consisted of a 0.9 μm GaN layer followed by a 25-nm-thick $Al_{0.09}Ga_{0.91}N$ barrier and a 3-nm-thick GaN cap layer.[12,13]

The polarization-induced 2DEG at the GaN/AlGaN interface exhibits high Hall mobility, of the order of $\mu_H = 75\,000$–$80\,000$ cm^2/V s, measured at 4.2 K, owing to the

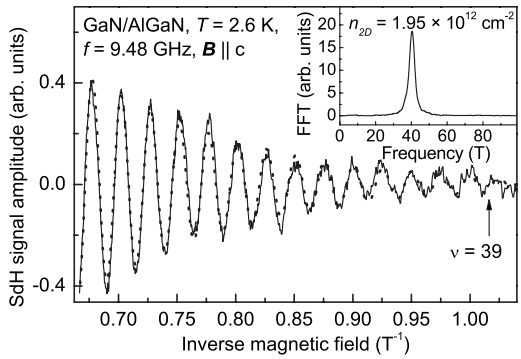

FIG. 1. Microwave-detected Shubnikov–de Haas oscillations measured for a GaN/AlGaN sample ($B||c$), solid line. Fit of Eq. (1) with T_D=1.25 K, dotted line. The background originating from a magnetoplasma resonance was subtracted. Inset: fast Fourier transform spectrum of the SdH signal. It shows one dominant oscillation frequency, corresponding to a sheet electron concentration of $n_{2D}=1.95\times10^{12}$ cm^{-2}.

high quality and low dislocation density of the substrate used. The screw dislocation density is typically as low as 10^4-10^5 cm^{-2} in these samples. The sheet carrier density amounts to $n_{2D}=2\times10^{12}$ cm^{-2}.

Properties of the 2DEG at the GaN/AlGaN interface were studied by standard microwave resonance spectrometry using a Bruker ELEXSYS E-580 ESR spectrometer. The spectrometer was operating at a frequency of f=9.48 GHz with a rectangular TE_{102} cavity, where the sample was placed in the maximum of the microwave magnetic field. Coupling to the cyclotron-plasmon modes occurs due to inevitable in-plane components of the microwave *electric field* owing to the finite sample size and fringe fields in the perturbed cavity. The temperature in the experiment was lowered down to 2 K using a continuous-flow Oxford cryostat. The static magnetic field $\boldsymbol{B}$ was swept up to 1.5 T.

III. EXPERIMENTAL RESULTS

A. Shubnikov–de Haas oscillations

As shown in Fig. 1, Shubnikov–de Haas (SdH) oscillations are observed due to non-resonant microwave absorption without any electrical contacts to the sample. Here, the magnetic field B was modulated with the amplitude of 5 G at 100 kHz. The modulation parameters were selected to avoid distortion of the SdH signal. Due to the modulation of the magnetic field, the spectra recorded represent the first derivative of the microwave absorption vs the magnetic field.

In Fig. 1, the measured Shubnikov–de Haas signal is plotted as a function of the inverse magnetic field B^{-1}. The spectrum depends only on the perpendicular component of the applied magnetic field (not shown in the figure), confirming the two-dimensional character of the observed spectrum. The onset of the oscillations occurs at a magnetic field of about 1 T, which corresponds to a Landau level filling factor as high as ν=39. Fast Fourier transform (FFT) of the signal vs the inverse magnetic field shows one dominant oscillation frequency F (see inset to Fig. 1) due to a single occupied electrical subband in the GaN quantum well. From the FFT peak position, we obtain a sheet electron concentration of $n_{2D}=1.95\times10^{12}$ cm^{-2} for this GaN/AlGaN sample ($n_{2D}=2eF/h$), in good agreement with Hall data obtained on a companion sample grown in the same process.

The amplitude of the SdH oscillations for low magnetic fields ($\hbar\omega_C \ll k_BT$) measured by the dc resistivity ρ is proportional to[15–17]

$$\rho(B) \sim \frac{\beta T}{B}\exp\left[-\frac{\beta(T+T_D)}{B}\right]\cos\left(2\pi\frac{hn_{2D}}{2e}\frac{1}{B}\right), \quad (1)$$

where $\beta=2\pi^2k_Bm^*/\hbar e$. Here, n_{2D} is the sheet electron concentration, m^* stands for the effective mass of the conduction electrons, which is $m^*=0.2m_0$ for GaN,[6,8,18] and T_D is the Dingle temperature related to the quantum mobility by $\mu_q=\pi/\beta T_D$.

The experimental data presented in Fig. 1 show oscillations of the ac conductivity measured at a frequency of $\omega=0.6\times10^{11}$ s^{-1}. In Ref. 19 it has been shown that Eq. (1) is also valid for the microwave-detected SdH effect (at low magnetic fields), resulting in values for the quantum mobility that are consistent with those of dc resistivity measurements.

The first derivative of Eq. (1) was fitted to the SdH spectrum recorded for a GaN/AlGaN sample, yielding a Dingle temperature of T_D=1.25 K, which corresponds to a quantum mobility of μ_q=8600 cm^2/V s. This value is by a factor of 9 smaller than the Hall mobility obtained from magnetotransport measurements (μ_H=75 000–80 000 cm^2/V s) and by a factor of 18 smaller than the cyclotron mobility determined in the resonance experiment (μ_{CR}=152 000 cm^2/V s), as will be presented in Sec. III B.

The quantum mobility μ_q, as determined from the magnetic field dependence of the amplitude of SdH oscillations, is usually lower than the transport mobility μ_H determined from Hall measurements. This is due to the fact that μ_q is related to the mean time a carrier remains in a particular state before being scattered to a different state, while the transport mobility is related to the mean time a carrier moves in a particular direction. Thus, in calculating quantum lifetimes all scattering events are weighted equally, while in the case of transport lifetimes weighting by a factor of $[1-\cos(\varphi)]$ (where φ is the scattering angle) has to be included. In other words, transport lifetimes emphasize the importance of large-over small-angle scattering events.[20]

The low-field amplitude of SdH oscillations is very sensitive to fluctuations of the Fermi level. It has been shown earlier for GaN/AlGaN heterostructures (grown on GaN templates prepared on sapphire substrates) that in the presence of fluctuations of the sheet electron density by as little as a few percent, the value of μ_q determined from the SdH oscillations is substantially lowered with respect to the true quantum mobility. In these samples, μ_q did not exceed 4000 cm^2/V s.[21] The higher value of μ_q=8600 cm^2/Vs determined for our homoepitaxial layers indicates higher homogeneity of the 2D electron gas. The obtained value for μ_q is also closer here to the actual quantum mobility.

The cyclotron mobility μ_{CR} deduced from a half-width at half maximum of the cyclotron resonance line has been re-

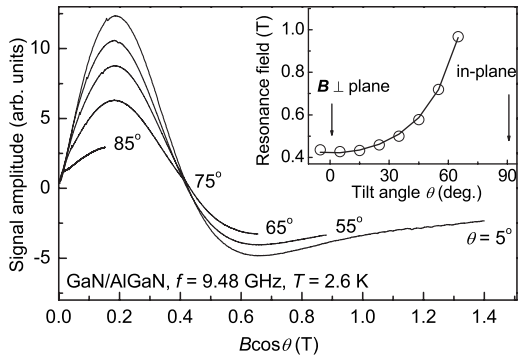

FIG. 2. Plasma-cyclotron resonances in GaN/AlGaN, measured at various angles θ between the external magnetic field B and the direction normal to the sample plane, are plotted as a function of $B\cos\theta$. Inset: resonance magnetic field vs tilt angle θ (points) following a $1/\cos\theta$ dependence (solid line).

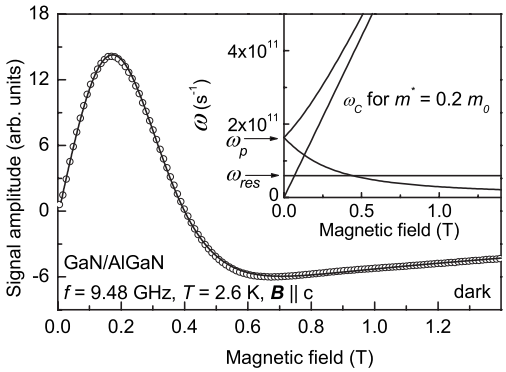

FIG. 3. Dots: First derivative of microwave absorption due to the plasmon-cyclotron resonance measured in a GaN/AlGaN sample (θ=0, sample dimension 3.5×4 mm^2). Some data points have been omitted for the clarity of the picture. Solid line: least squares fit of Eq. (6) with the best fit parameters listed in Table I. The inset shows the upper and the lower branch of the coupled plasma-cyclotron resonance calculated according to Eq. (2). The arrows mark plasma and microwave frequencies.

cently investigated for GaN/AlGaN samples having a sheet electron concentration in the range of $(1-4.5)\times10^{12}$ cm^{-2} and transport mobilities of 10 000–40 000 cm^2/V s.[21] It has been shown that μ_{CR} coincides with the transport mobility μ_H for lower electron densities, while for higher densities μ_{CR} becomes much lower than the μ_H. The cyclotron mobility has been identified with the quantum mobility, and the discrepancy at higher electron densities has been attributed to dominant large-angle scattering in the samples investigated. It appears rather natural, however, to equate cyclotron and transport mobilities, as they both arise from the same Drude formalism. Then, the discrepancy between μ_{CR} and μ_H observed at higher sheet electron densities should be accounted for by other mechanisms broadening the cyclotron resonance line, e.g., electron-electron interaction and inhomogeneities in the sample. In any case, $n_{2D}=2\times10^{12}$ cm^{-2}, which is the concentration of our homoepitaxial samples, is still in the range where μ_{CR} and μ_H give the same values in Ref. 21. In our experiment, however, we still observe a discrepancy (μ_{CR} is higher than μ_H), which will be discussed in Sec. III B.

Sample illumination changes the carrier concentration, which also leads to a change of the μ_{CR} and μ_q. Details are described in Sec. III B.

B. Line shape of the coupled plasmon-cyclotron resonance

Figure 2 shows a strong electric dipole-type resonance (first derivative of microwave absorption) recorded in a GaN/AlGaN sample. The spectra were measured for various orientations of the magnetic field $\boldsymbol{B}$, clearly showing a common dependence on the *perpendicular component* of the applied field, $B\cos\theta$, as is usual for two-dimensional electrons. Here, θ is the angle between $\boldsymbol{B}$ and the GaN c axis, which is perpendicular to the sample plane. The resonance position of the observed line is shifted, however, toward higher magnetic fields, $B\cos\theta$=0.42 T, with respect to the pure cyclotron resonance expected for the cyclotron mass of GaN electrons, $B\cos\theta$=0.07 T. Such a shift may originate from the coupling of the cyclotron motion to plasma oscillations.[1–5,22]

It has been observed, e.g., for GaAs-based 2D heterostructures, that the cyclotron motion of an electron and the plasma oscillations hybridize when the frequencies of the two modes approach each other. The two resonance frequencies for plasmon-cyclotron coupling, the upper cyclotronlike branch and the lower edge mode, are then given by[2,22]

$$\omega_{res}^{\pm} = \pm\frac{\omega_c}{2} + \sqrt{\omega_p^2 + \left(\frac{\omega_c}{2}\right)^2}, \tag{2}$$

where ω_C stands for the cyclotron frequency and ω_p is the plasma frequency, which scales with the plasmon wave vector and thus with the sample size. For a disk-shaped sample with a radius R, this relation is given by[4,23]

$$\omega_p^2 = \frac{n_{2D}e^2}{m^*(1+\varepsilon)\varepsilon_0 R}. \tag{3}$$

Here, n_{2D} is the sheet electron concentration, ε_0 the vacuum permittivity, and ε a static dielectric constant, which equals 10.4 for GaN.[24] The dependence of the coupled plasmon-cyclotron resonance frequencies on the magnetic field is plotted in the inset in Fig. 3.

It may be worthwhile to note here that Eq. (2) leads to a $1/\cos\theta$ dependence of the resonance magnetic field, as it is a case of a pure cyclotron resonance. It is thus not possible to distinguish pure cyclotron resonance and the plasmon-cyclotron coupling only from the angular analysis. For plasmon-cyclotron coupling, the resonance position (for the edge mode) is shifted toward higher magnetic fields, and the shift depends on both the sample size and the sheet electron concentration.

For a sample with a rectangular shape, two different plasma frequencies exist, which are related to the sample length and width. These modes are coupled in the presence of a magnetic field. In our experiment, we had rectangular samples. Due to the orientation of the sample inside the microwave cavity, however, the applied linear polarized micro-

wave electric field was always perpendicular to the longer edge of a sample, so that only one plasma frequency related to the smaller sample dimension could be excited here. To analyze the recorded resonance, we have thus used a one-mode approximation, which, as shown below, gives a good agreement with experimental results.

To describe the line shape of the ac electric absorption of the coupled resonance recorded in our GaN/AlGaN heterostructures, we assumed a Lorentzian dependence for the absorption of circular polarized electromagnetic waves in the frequency domain, with the two resonance frequencies given by Eq. (2),

$$F^{\pm}(\omega,B) = \frac{A\tau_C}{\pi}\frac{1}{1+\tau_C^2[\omega-\omega_{res}^{\pm}(B)]^2}, \tag{4}$$

for σ^+ (cyclotron resonance active) and σ^- (cyclotron resonance inactive) polarization, respectively.[22] The function decribed by Eq. (4) reflects the ac Drude conductivity,[6] where the scattering time τ_C is related to the mobility μ_{CR} by the relation

$$\mu_{CR} = \frac{e}{m^*}\tau_C. \tag{5}$$

In order to fit the shape of the line recorded in our resonance experiment, we need to take into account the linear polarization of the absorbed microwaves and the fact that we measure the first derivative of the absorption vs magnetic field due to the use of modulation of B and lock-in detection. We treat the linear polarization as a sum of σ^+ and σ^- polarization. This leads to a final expression, which reproduces the characteristic asymmetric line shape of the magnetoplasma resonance in the magnetic field domain,

$$f(\omega,B) = \frac{1}{2}\frac{\partial}{\partial B}[F^+(\omega,B)+F^-(\omega,B)]. \tag{6}$$

Figure 3 shows a fit of Eq. (6) to the spectrum recorded at $\theta=0$. The best fit parameters in this case are $\omega_p = (1.63\pm0.1)\times10^{11}$ s^{-1} and $\tau_C=(1.73\pm0.1)\times10^{-11}$ s^{-1}, which correspond to $\mu_{CR}=(152\,000\pm8000)$ cm^2/V s. The microwave frequency was set to the experimental value of $\omega_{res}=0.6\times10^{11}$ s^{-1}.

The inset in Fig. 3 shows two branches of magnetoplasma modes calculated according to Eq. (2) with parameters obtained from the fit. As can be clearly seen, the fitted plasma frequency is substantially higher than the microwave frequency, so the main contribution to the line shape of the observed resonance originates from the edge magnetoplasma branch. Due to the finite width of the resonance line, the cyclotronlike branch contributes slightly to the spectrum for magnetic fields close to $B=0$.

The obtained cyclotron mobility is by a factor of 2 higher than the transport mobility determined from a Hall experiment. As argued in Sec. III A the cyclotron resonance in the GaN/AlGaN heterostructure should give a cyclotron mobility close to that detemined from transport, at least for samples with low sheet electron concentration.[21] The discrepancy between the two mobilities values observed in our experiment can be explained in terms of an ac character of the cyclotron resonance measurement, which becomes more pronounced for high-mobility samples. The main contribution of the electron gas (oscillating at the resonance frequency $\omega_{res}=0.6\times10^{11}$ s^{-1}) stems from electrons confined in high-quality areas of the sample, where scattering potentials originating from residual and remote impurities are well screened. The mobility measured here in a cyclotron resonance experiment can thus be closer to the value limited by intrinsic properties of the GaN host crystal, namely, by acoustic phonon scattering. Moreover, the interpretation of dc conductivity measurements assumes a uniform current distribution. When the current is not uniform, e.g., due to long range potential fluctuations, the resulting Hall mobility is smaller than that corresponding to the scattering time.

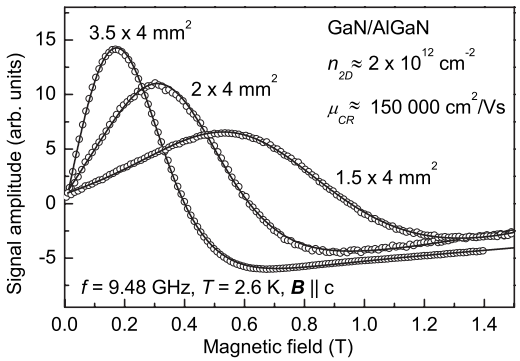

FIG. 4. Plasmon-cyclotron resonance in GaN/AlGaN with different sample dimensions but the same sheet electron concentration and mobility. Dots are experimental data, with some data points omitted for clarity. The solid lines represent least squares fits of Eq. (6) with best fit parameters listed in Table I.

C. Dependence of the plasmon-cyclotron resonance on the sample size

The plasma frequency in a 2D electron gas depends on the sample dimensions, as expected according to Eq. (3). To show that the observed resonance in GaN/AlGaN is really sample size dependent, we have measured a set of samples cleaved from the same wafer, having equal sheet electron concentrations and mobilities but different sizes. The three samples measured had an approximately rectangular shape, with their bigger dimension equal to about 4 mm (plasma oscillations related to this dimension are not excited in our experiment) and the smaller one equal to 3.5, 2.0, and 1.5 mm. The results are shown in Fig. 4. Indeed, with decreasing sample size, the resonance is shifted toward higher magnetic fields, reflecting an increase of the plasma frequency. All spectra can be fitted with very good precision using Eq. (6), supporting the assignment to the magnetoplasma resonance. The best fit parameters for all samples are listed in Table I. The obtained $\tau_C=\text{const}=(1.8\pm0.1)\times10^{-11}$ s, while ω_p is size dependent.

From the fitted plasma frequencies, taking the sheet electron concentration equal to $n_{2D}=1.95\times10^{12}$ cm^{-2}, we can

TABLE I. Transport parameters for GaN/AlGaN heterostructures obtained from the Shubnikov–de Haas oscillations (n_{2D} and μ_q) and from the analysis of the plasmon-cyclotron resonance line shape (ω_p, τ_C, and μ_{CR}).

Sample size (mm^2)	Illumination	n_{2D} (cm^{-2})	μ_q ($cm^2/V\,s$) ± 500	ω_p (s^{-1}) $\pm 0.1\times10^{11}$	τ_C (s) $\pm 0.1\times10^{-11}$	μ_{CR} ($cm^2/V\,s$) ± 8000
3.5×4	Dark	$(1.95\pm0.05)\times10^{12}$	8600 ± 500	1.63×10^{11}	1.73×10^{-11}	152000
2.0×4	Dark			1.98×10^{11}	1.89×10^{-11}	166000
1.5×4	Dark			2.58×10^{11}	1.74×10^{-11}	153000
3.5×4	White	$(2.2\pm0.1)\times10^{12}$	4300 ± 1000	1.75×10^{11}	1.53×10^{-11}	135000
3.5×4	UV	$(3.5\pm0.1)\times10^{12}$	2900 ± 1000	2.45×10^{11}	1.18×10^{-11}	104000
3.5×4	Dark after UV			2.27×10^{11}	1.34×10^{-11}	118000

calculate the effective diameter of the measured samples using Eq. (3). We obtain $2R_{eff}=2$, 1.46, and 0.84 mm, which are comparable to the actual widths of the sample (3.5, 2.0, and 1.5 mm, respectively), but some discrepancies are clearly visible. The observed discrepancy may be accounted for considering the nonradial sample geometry and the fact that the 2DEG may not occupy the whole area of the measured sample.

The frequency f of the magnetoplasma oscillations for a *millimeter-sized* sample with a sheet electron density of 2×10^{12} cm^{-2} is of the order of a few GHz. Reducing the sample dimensions down to the micrometer regime, the plasma frequency is expected to fall into the THz region, which can be interesting for the generation or detection of the THz radiation.[25] Making use of the plasmon-cyclotron coupling, the resonance frequency can be further tuned toward both higher and lower frequencies by applying relatively low magnetic fields. The properties of GaN-based heterostructures have already been successfully used in blue optoelectronics as well as in high-power and high-temperature electronics. Here, we see that they can be also considered as a promising candidate for the THz technology.

D. Influence of illumination

It is widely recognized that a 2DEG is present at the GaN/AlGaN interface even without any intentional doping due to the presence of strong polarization fields in the heterostructure. Native defects from the surface of the AlGaN barrier have been proposed as a source of the two-dimensional electrons in the GaN quantum well.[26] There, it has been calculated that the polarization fields are pushing native defect levels above the Fermi level, promoting transfer of electrons from localized defect states at the surface to the triangle well at the interface.

It has been also shown that illumination, which affects the charge distribution in the GaN/AlGaN heterostructure, simultaneously influences the electron concentration in the 2D channel and the surface barrier height.[27] Under ultraviolet illumination, the 2D electron concentration can be increased and the surface barrier height is reduced. This effect was explained in terms of migration of holes, photogenerated at the AlGaN barrier, toward the surface and the accumulation of photogenerated electrons at the GaN/AlGaN interface. Photoionization of localized defect states in the AlGaN barrier can be also considered as a source of excess electrons in the quantum well. Slow recombination of the photocarriers has been observed due to the charge separation by the AlGaN barrier width and possibly due to capturing by impurities localized in the barrier.

In order to vary the electron concentration in the 2D channel, the GaN/AlGaN sample (3.5×4 mm^2) was illuminated in the spectrometer cavity and the resonance spectra were recorded. The sheet electron concentration under illumination was monitored by measuring the SdH oscillations. This approach allowed us to test the applied model of the plasmon-cyclotron coupling without changing the sample dimensions. Experimental data are shown in Fig. 5.

Illumination with a white halogen lamp light led to a slow increase of the electron concentration. After 15 min of illumination, the 2D concentration increased from 1.95×10^{12} to 2.2×10^{12} cm^{-2}, and the effect did not saturate. Illumination with infrared light had almost no influence on n_{2D}, while illumination with UV laser light (multiline 351 and 363 nm) increased drastically the concentration up to 3.5×10^{12} cm^{-2}. After switching off the UV illumination, the concentration slowly came back to its "dark" value, reaching $n_{2D}=3\times10^{12}$ cm^{-2} after 10 min. The observed response of the sample is consistent with results described in Ref. 27.

Figure 5(a) shows the fast Fourier transform spectra of the measured Shubnikov–de Haas oscillations in the dark and under illumination. The shift of the FFT peak toward higher frequencies under illumination is clearly visible, together with the broadening of the FFT line, which may suggest a decrease of the mobility. Indeed, fitting Eq. (1) to the SdH spectra obtained under illumination reveals a drop of the quantum mobility from $\mu_q=8600$ $cm^2/V\,s$ in the dark down to $\mu_q=2900$ $cm^2/V\,s$ under the UV illumination (see Table I).

Plasmon-cyclotron resonances recorded simultaneously with the SdH oscillations in the illumination experiment are shown in Fig. 5(b). With increasing sheet electron concentration (under illumination), the edge magnetoplasma resonance moves toward higher magnetic fields, reflecting an increase of the plasma frequency, as described by Eq. (2).

Figure 6 shows all data collected in the illumination experiment. The upper panel shows the square of the plasma

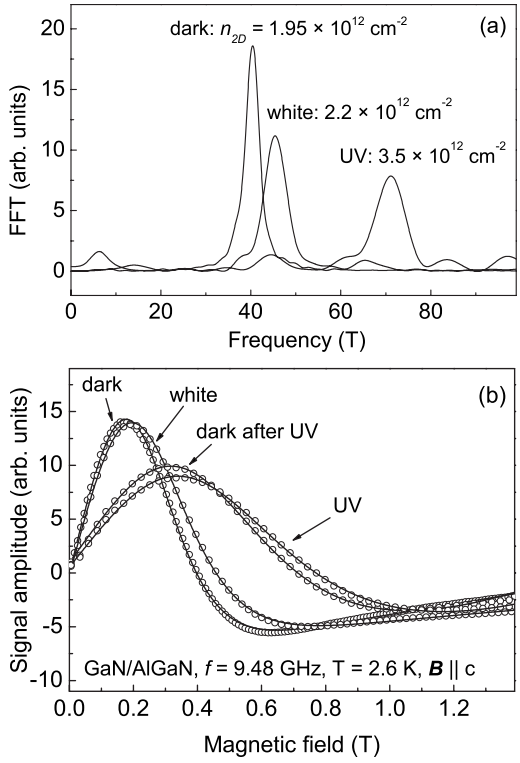

FIG. 5. Illumination experiment. (a) Fast Fourier transform of the Shubnikov–de Haas signal in a GaN/AlGaN sample, measured in the dark and under white halogen lamp or UV laser light illumination. (b) Coupled plasma-cyclotron resonance measured simultaneously in the same experiment. Dots are experimental, with some data points omitted for the clarity. Solid lines represent fits of Eq. (6) with best fit parameters listed in Table I.

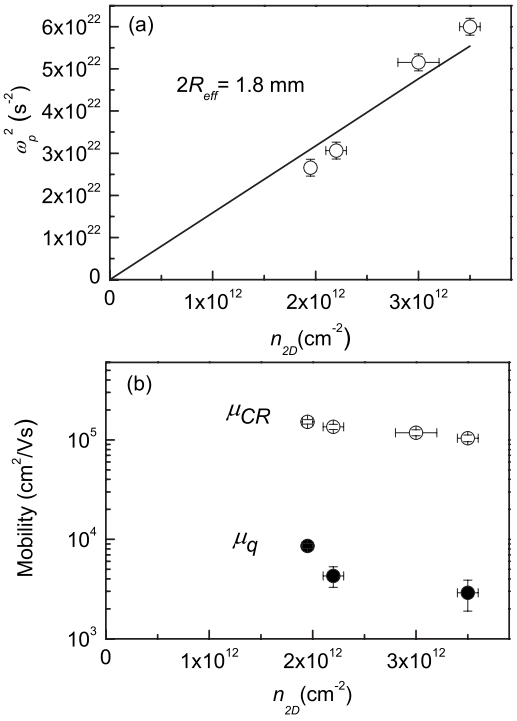

FIG. 6. (a) The square of the plasma frequency determined from plasmon-cyclotron resonance versus the sheet electron concentration obtained from the SdH oscillations for a GaN/AlGaN sample with a width of 3.5 mm. The solid line represents a fit of Eq. (3), yielding an effective diameter of the sample equal to $2R_{eff}$ = 1.8 mm. (b) Quantum and cyclotron mobilities determined from the SdH oscillations and from the magnetoplasma linewidth, respectively.

frequency obtained from the fit of the magnetoplasma line shape vs the sheet electron concentration obtained from the Fourier transform of the SdH signal. A linear dependence is consistent with Eq. (3). The slope of $\omega_p(n_{2D})$ corresponds to the effective diameter of the sample equal to $2R_{eff}$ = 1.8±0.2 mm.

Figure 6(b) shows the cyclotron and the quantum mobilities obtained from the magnetoplasma linewidth and from the magnetic field dependence of the SdH oscillations, respectively, vs the sheet electron concentration. Both mobilities decrease with increasing n_{2D}. However, the drop of μ_{CR} is much smaller than that of μ_q. The μ_{CR}/μ_q ratio equals 18 in the dark and 36 under the UV illumination.

As discussed above, illumination increases both the sheet electron concentration in the GaN 2D channel and the concentration of ionized defects in the AlGaN barrier. The increased number of remote scattering centers in the barrier can be responsible for the drop of both mobility values, μ_{CR} and μ_q, observed in the experiment. On the other hand, the increase of the sheet electron concentration in the well is followed by the enlargement of the screening radius, which leads to a longer characteristic length of potential fluctuations. This can explain the significant increase of the μ_{CR}/μ_q ratio.

IV. CONCLUSIONS

To summarize, we observed coupling of plasma oscillations to the cyclotron motion, an edge magnetoplasma mode, in the high-mobility 2D electron gas confined at the GaN/AlGaN interface using microwave resonance spectrometry in a conventional ESR spectrometer. We have shown that the analysis of the coupled plasmon-cyclotron resonance provides a *contactless* method to characterize electronic properties of the 2D electron gas. Both the sheet electron concentration and the mobility can be determined with high precision from the resonance position and the line shape of coupled magnetoplasma modes, for which we have derived a simple formula based on the theory for dimensional resonances.[2,22]

We also observed Shubnikov–de Haas oscillations in GaN/AlGaN using the microwave resonance spectroscopy. SdH oscillations have been investigated earlier by this method, e.g., for InGaAs and AlGaAs quantum wells.[28–30] The observation failed, however, for high-mobility Si-based heterostructures, in which large potential fluctuations are present.[31]

The observation of the plasmon-cyclotron coupling was possible, thanks to the high mobility of the electrons

confined at the GaN/AlGaN heterojunction in the investigated samples. High mobility was achieved here due to the optimization of the MBE-growth technique, allowing us to obtain a high-quality interface between GaN and AlGaN, as well as the use of a native GaN substrate, which resulted in low dislocation density in the heterostructure.

ACKNOWLEDGMENTS

This work has been supported by the Fonds zur Förderung der Wissenschaftlichen Forschung, Austria, the ÖAD and GMe (all Vienna), and by the funds for science 2007-2010 as a research project PBZ/MNiSW/07/2006/39, Poland.

[1] T. N. Theis, J. P. Kotthaus, and P. J. Stiles, Solid State Commun. **24**, 273 (1977).
[2] S. J. Allen, Jr., H. L. Stormer, and J. C. M. Hwang, Phys. Rev. B **28**, 4875 (1983).
[3] I. V. Kukushkin, J. H. Smet, K. von Klitzing, and W. Wegscheider, Nature (London) **415**, 409 (2002).
[4] I. V. Kukushkin, J. H. Smet, S. A. Mikhailov, D. V. Kulakovskii, K. von Klitzing, and W. Wegscheider, Phys. Rev. Lett. **90**, 156801 (2003).
[5] B. M. Ashkinadze and V. I. Yudson, Phys. Rev. Lett. **83**, 812 (1999).
[6] W. Knap, H. Alause, J. M. Bluet, J. Camassel, J. Young, M. Asif-Khan, Q. Chen, S. Huant, and M. Shur, Solid State Commun. **99**, 195 (1996).
[7] Y. J. Wang, R. Kaplan, H. K. Ng, K. Doverspike, D. K. Gaskill, T. Ikedo, I. Akasaki, and H. Amono, J. Appl. Phys. **79**, 8007 (1996).
[8] W. Knap, S. Contreras, H. Alause, C. Skierbiszewski, J. Camassel, M. Dyakonov, J. L. Robert, J. Yang, Q. Chen, M. Asif-Khan, M. L. Sadowski, S. Huant, F. H. Yang, M. Goiran, J. Leotin, and M. S. Shur, Appl. Phys. Lett. **70**, 2123 (1997).
[9] S. Syed, M. J. Manfra, Y. J. Wang, H. L. Stormer, and R. J. Molnar, Phys. Rev. B **67**, 241304(R) (2003).
[10] Z.-F. Li, W. Lu, S. C. Shen, S. Holland, C. M. Hu, D. Heitmann, B. Shen, Y. D. Zheng, T. Someya, and Y. Arakawa, Appl. Phys. Lett. **80**, 431 (2002).
[11] G. Abstreiter, J. P. Kotthaus, and J. F. Koch, Phys. Rev. B **14**, 2480 (1976).
[12] C. Skierbiszewski, Z. Wasilewski, M. Siekacz, A. Feduniewicz, B. Pastuszka, I. Grzegory, M. Leszczynski, and S. Porowski, Phys. Status Solidi A **201**, 320 (2004).
[13] C. Skierbiszewski, K. Dybko, W. Knap, M. Siekacz, J. Lusakowski, W. Krupczynski, G. Nowak, M. Bockowski, Z. R. Wasilewski, D. Maude, T. Suski, and S. Porowski, Appl. Phys. Lett. **86**, 102106 (2005).
[14] S. Krukowski, M. Bockowski, B. Lucznik, I. Grzegory, S. Porowski, T. Suski, and Z. Romanowski, J. Phys.: Condens. Matter **13**, 8881 (2001).
[15] T. Ando, A. B. Fowler, and F. Stern, Rev. Mod. Phys. **54**, 437 (1982).
[16] S. Yamada and T. Makimoto, Appl. Phys. Lett. **57**, 1022 (1990).
[17] E. Skuras, R. Kumar, R. L. Williams, R. A. Stradling, J. E. Dmochowski, E. A. Johnson, A. Mackinnon, J. J. Harris, R. B. Beall, C. Skierbiszewski, J. Singleton, P. J. van der Wel, and P. Wisniewski, Semicond. Sci. Technol. **6**, 535 (1991).
[18] P. Perlin, E. Litwin-Staszewska, B. Suchanek, W. Knap, J. Camassel, T. Suski, R. Piotrzkowski, I. Grzegory, S. Porowski, E. Kamińska, and J. C. Chervin, Appl. Phys. Lett. **68**, 1114 (1996).
[19] H. Linke, P. Omling, P. Ramvall, B. Meyer, M. Drechsler, C. Wetzel, R. Rudeloff, and F. Scholz, J. Appl. Phys. **73**, 7533 (1993).
[20] L. Hsu and W. Walukiewicz, Appl. Phys. Lett. **80**, 2508 (2002).
[21] S. Syed, M. J. Manfra, Y. J. Wang, R. J. Molnar, and H. L. Stormer, Appl. Phys. Lett. **84**, 1507 (2004).
[22] E. D. Palik and J. K. Furdyna, Rep. Prog. Phys. **33**, 1193 (1970).
[23] A. L. Fetter, Phys. Rev. B **33**, 5221 (1986).
[24] A. S. Barker, Jr. and M. Ilegems, Phys. Rev. B **7**, 743 (1973).
[25] W. Knap, J. Lusakowski, T. Parenty, S. Bollaert, A. Cappy, V. V. Popov, and M. S. Shur, Appl. Phys. Lett. **84**, 2331 (2004).
[26] L. Hsu and W. Walukiewicz, J. Appl. Phys. **89**, 1783 (2001).
[27] G. Koley, Ho-Young Cha, Jeonghyun Hwang, W. J. Schaff, L. F. Eastman, and M. G. Spencer, J. Appl. Phys. **96**, 4253 (2004).
[28] G. Hendorfer, M. Seto, H. Ruckser, W. Jantsch, M. Helm, G. Brunthaler, W. Jost, H. Obloh, K. Kohler, and D. J. As, Phys. Rev. B **48**, 2328 (1993).
[29] W. Timelthaler, W. Jantsch, and G. Weimann, Semicond. Sci. Technol. **5**, 686 (1990).
[30] P. Omling, B. Meyer, and P. Emanuelsson, Appl. Phys. Lett. **58**, 931 (1991).
[31] Z. Wilamowski, N. Sandersfeld, W. Jantsch, D. Tobben, and F. Schaffler, Phys. Rev. Lett. **87**, 026401 (2001).